JACS
JOURNAL OF THE AMERICAN CHEMICAL SOCIETY
Article
pubs.acs.org/JACS

Magnetic Blocking at 10 K and a Dipolar-Mediated Avalanche in Salts of the Bis(η^8-cyclooctatetraenide) Complex $[Er(COT)_2]^-$

Katie R. Meihaus and Jeffrey R. Long*

Department of Chemistry, University of California, Berkeley, California 94720, United States

Supporting Information

ABSTRACT: The structures and magnetic properties of $[K(18\text{-crown-6})]^+$ (**1**) and $[K(18\text{-crown-6})(THF)_2]^+$ (**2**) salts of the η^8-cyclooctatetraenide sandwich complex $[Er(COT)_2]^-$ (COT^{2-} = cyclooctatetraene dianion) are reported. Despite slight differences in symmetry, both compounds exhibit slow magnetic relaxation under zero applied dc field with relaxation barriers of ~150 cm^{-1} and waist-restricted magnetic hysteresis. Dc relaxation and dilution studies suggest that the drop in the magnetic hysteresis near zero field is influenced by a bulk magnetic avalanche effect coupled with tunneling of the magnetization. Through dilution with $[K(18\text{-crown-6})(THF)_2][Y(COT)_2]$ (**3**), these phenomena are substantially quenched, resulting in an open hysteresis loop to 10 K. Importantly, this represents the highest blocking temperature yet observed for a mononuclear complex and the second highest for any single-molecule magnet. A comprehensive comparative analysis of the magnetism of $[K(18\text{-crown-6})][Ln(COT)_2]$ (Ln = Sm, Tb, Dy, Ho, Yb) reveals slow relaxation only for $[K(18\text{-crown-6})][Dy(COT)_2]$ (**4**) with weak temperature dependence. Collectively, these results highlight the utility of an equatorial ligand field for facilitating slow magnetic relaxation in the prolate Er^{III} ion.

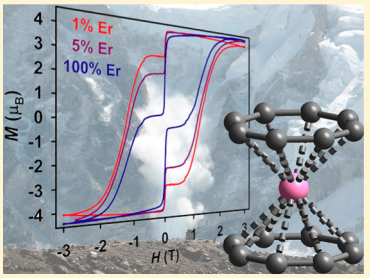

INTRODUCTION

Molecular magnetism has made great strides following the characterization of the first lanthanide-based single-molecule magnets $[LnPc_2]^-$ (Ln = Tb, Dy; Pc^{2-} = phthalocyanine dianion).[1] In conjunction with several important computational and theoretical efforts,[2] the discovery of a host of intriguing new 4f-element systems[3] continues to drive understanding of factors that dictate slow magnetic relaxation. Notwithstanding many important recent discoveries of systems incorporating d-block[4] and 5f-elements,[5] the 4f-elements remain largely unsurpassed in their utility for the design of molecular magnets, due to their large moments and inherent magnetic anisotropy. Notably, some of the highest relaxation barriers to date in lanthanide-containing species are still observed for mononuclear complexes,[6] in part due to the difficulty of assembling multinuclear structures with cooperative exchange interactions[3e,7] and also of engineering strong coupling between lanthanides centers without the aid of radical bridges.[8] While recently a multinuclear cluster containing Dy^{III} was shown to possess an impressive barrier in excess of 585 cm^{-1}, the slow relaxation is ultimately single-ion in origin.[3g]

A preeminent feature of mononuclear lanthanide magnets is their tunability, which allows for increased control over structure, and therefore magnetic properties, when compared to multinuclear species. Symmetry is also a key parameter that is important in dictating the M_J ground state, possible mixing of the M_J levels, and therefore the relaxation behavior that will be observed.[2a,d,3e,9] Considering this, we were intrigued by the discovery of ErCp*(COT) ($[Cp^*]^-$ = pentamethylcyclopentadienide anion), where Er^{III} is coordinated by one η^8-cyclooctatetraenide ligand and one η^5-pentamethylcyclopentadienide ligand. Despite its low symmetry, ErCp*(COT) demonstrates a large relaxation barrier and magnetic hysteresis up to 5 K.[10] The origin of this slow relaxation was found to derive from an Ising ground state of $M_J = {}^{15}/_2$ that is well-separated from an $M_J = {}^{13}/_2$ excited state, as determined by modeling dc susceptibility assuming a molecular symmetry of $C_{\infty v}$. Very recently, angular-resolved magnetometry experiments have elegantly confirmed easy-axis anisotropy in ErCp*(COT).[11] From an electrostatic standpoint, it could be argued that the well-isolated M_J ground state stems from the arrangement of the π-bonding molecular orbitals of the COT^{2-} and $[Cp^*]^-$ ligands, which should provide a predominantly equatorial ligand field, favoring stabilization of the most prolate $M_J = {}^{15}/_2$ state of Er^{III}. Indeed, very recently ab initio calculations have demonstrated[12] that in the (symmetrized) homoleptic complex $[Dy(COT)_2]^-$, the ligand field is more equatorial than axial.[9] Given the relaxation behavior demonstrated by ErCp*(COT), we were motivated to investigate the homoleptic cyclooctatetraenide species $[Er(COT)_2]^-$, an ideal target for the observation of slow magnetic relaxation given its more symmetric equatorial ligand field.

EXPERIMENTAL SECTION

General Considerations. All reactions and subsequent manipulations were performed under anaerobic and anhydrous conditions in a nitrogen-atmosphere glovebox. Tetrahydrofuran (THF) and hexanes were dried by passage over activated molecular sieves using a custom-built solvent system. Anhydrous $LnCl_3$ was purchased from Strem Chemicals, and cyclooctatetraene and 18-crown-6 were purchased

Received: September 12, 2013
Published: November 4, 2013

   dx.doi.org/10.1021/ja4094814 | J. Am. Chem. Soc. 2013, 135, 17952−17957

from Sigma Aldrich. All chemicals were used as received. ^{1}H NMR spectra were recorded on a Bruker AV 600 spectrometer. Elemental analyses were performed by the Micro-Mass Facility at the University of California, Berkeley on a Perkin-Elmer 2400 Series II combustion analyzer. Quartz tubes used for magnetic samples were custom-made by D&G Glassblowing, Inc.

Synthesis. K_2COT was prepared from modification of the original method of Katz,[13] whereupon an excess of 2 equiv of potassium metal was added to a stirring solution of cyclooctatetraene in THF. Over the course of 24 h, the pale yellow cyclooctatetraene solution took on a dark yellow-brown color, indicative of the dianion formation. After filtering off excess potassium metal, concentration of the resulting solution and storage at −34 °C resulted in formation of large transparent beige crystals of K_2COT, which were used in subsequent reactions.

$K[Ln(COT)_2]$ (Ln = Er, Sm, Tb, Dy, Ho, Yb, Y) was prepared by modification of the literature procedure.[14] To a stirring slurry of $LnCl_3$ in THF was added dropwise a chilled (−34 °C) solution of K_2COT in THF. After stirring for 3 h, the reaction mixture was allowed to settle and a cloudy precipitate filtered over a layer of Celite (4 cm). After removal of the solvent in vacuo, yellow (Er, Tb, Dy, Ho), brown (Sm), dark blue (Yb), and pale yellow-green (Y) powders were isolated.

$K[Er(COT)_2]$. $ErCl_3$ (221.6 mg, 0.8099 mmol) in THF (4 mL) was combined with K_2COT (295.3 mg, 1.619 mmol) in THF (4 mL) as described above. The yellow solution quickly took on a cloudy appearance. After stirring for 3 h, the solution was filtered and dried to obtain 228.7 mg of microcrystalline $K[Er(COT)_2]$ (68.1% yield). A proton NMR spectrum collected on this powder in THF-d_8 displayed a single broad peak at −88.8 ppm.

$[K(18\text{-c-}6)(THF)_2][Ln(COT)_2]$. Addition of 1 equiv of 18-crown-6 to $K[Ln(COT)_2]$ and recrystallization from concentrated THF resulted in the formation of $[K(18\text{-c-}6)(THF)_2][Ln(COT)_2]$ for Y (**3**), Dy (**4**), and Sm. In the case of Er, complex **1** was isolated, $[K(18\text{-c-}6)][Er(COT)_2]\cdot 2THF$, containing an inner-sphere potassium counterion (Tb, Ho, and Yb congeners were found to be isostructural with **1**). Treatment of **1** with an additional equivalent of 18-crown-6 and recrystallization from concentrated THF at −34 °C resulted in crystals of **2**, $[K(18\text{-c-}6)(THF)_2][Er(COT)_2]$. Elemental Analysis. Compound **1**: Calcd for $ErC_{28}H_{40}O_6K$ (%) C: 49.53, H: 5.95. Found (%): C, 49.67; H, 6.01. Compound **2**: Calcd for $ErC_{28}H_{40}O_6K$ (%): C, 49.53; H, 5.95. Found (%): C, 49.53; H, 5.83.

Crystallography. Crystals were mounted on Kapton loops and transferred to a Brüker SMART APEX diffractometer, cooled in a nitrogen stream. The SMART program package was used to determine the unit cell parameters and for data collection (10 s/frame scan time for a hemisphere of diffraction data). Data integration was performed by SAINT and the absorption correction provided by SADABS. Subsequent calculations were carried out using the WinGX program. The structures were solved by direct methods and refined against *F*2 by full-matrix least-squares techniques. The analytical scattering factors for neutral atoms were used throughout the analysis. Hydrogen atoms were included using a riding model. Full crystal data is presented for complexes **1**−**4** and $[K(18\text{-crown-}6)][Sm(COT)_2]$. In the case of Tb, Ho, and Yb^{III} analogues, unit cell data revealed these to be isostructural with **1**. In the case of **1**, one of the COT^{2-} rings is disordered over staggered and eclipsed positions, and for **3** and $[K(18\text{-crown-}6)][Sm(COT)_2]$, one 18-crown-6 molecule is severely disordered. Thus, the corresponding carbon atoms were left isotropic during refinement.

Magnetic Measurements. Magnetic samples were prepared by adding crystalline powder compound to a 7 mm quartz tube with raised quartz platform. Solid eicosane was added to cover the samples to prevent crystallite torqueing and provide good thermal contact between the sample and the bath. The tubes were fitted with Teflon sealable adapters, evacuated using a glovebox vacuum pump, and flame-sealed under static vacuum. Following flame sealing, the solid eicosane was melted in a water bath held at 40 °C.

Magnetic susceptibility measurements were collected using a Quantum Design MPMS2 SQUID magnetometer. Dc susceptibility data measurements were performed at temperatures ranging from 1.8 to 300 K, using an applied field of 1000 Oe. Dc relaxation measurements were performed starting at fields of 5 and 1 T. The amount of paramagnetic species present in dilute samples was determined by adjusting the mass of the paramagnetic material until the low temperature portions of the dilute dc susceptibility curves overlapped with that of the neat compound. Ac magnetic susceptibility measurements were performed using a 4 Oe switching field. All data for **1**−**4** were corrected for diamagnetic contributions from the core diamagnetism estimated using Pascal's constants[15] to give χ_D = −0.0003438 emu/mol (**1** and **2**), −0.0003378 emu/mol (**3**), −0.0003448 emu/mol (**4**), and −0.00024306 emu/mol (eicosane). Cole−Cole plots were fitted using formulas describing χ_M' and χ_M'' in terms of frequency, constant temperature susceptibility (χ_T), adiabatic susceptibility (χ_S), relaxation time (τ), and a variable representing the distribution of relaxation times (α).[16] All data could be fitted to give $\alpha \leq 0.31$ in the case of **4** and $\alpha \leq 0.09$ in the case of **1** and **2**.

RESULTS AND DISCUSSION

The synthesis of $K[Ln(COT)_2]$ was originally pioneered in 1973 by Streitwieser;[14] however, this work did not report the Er^{III} congener and it was over three decades before characterization of the first homoleptic complex $[Er(COT)_2]^-$, isolated as a 1,3-diisopropylimidazolium ($[(N\text{-}^iPr)_2Im]^+$) salt.[17] The potassium salt of the $[Er(COT)_2]^-$complex reported here was synthesized by a modification of the published method for other lanthanides,[14] via slow addition of a THF solution of K_2COT at −34 °C to a stirring slurry of $ErCl_3$ in THF. When combined with 1 equiv of 18-crown-6, crystals of $[K(18\text{-c-}6)][Er(COT)_2]\cdot 2THF$ (**1**) formed over the course of 3−5 days from a concentrated THF solution stored at −34 °C. X-ray analysis of a single crystal revealed a triple-decker sandwich structure, with an $[Er(COT)_2]^-$ complex capped by an $[K(18\text{-crown-}6)]^+$ unit (Figure 1, left). Compound **1** crystallizes in the orthorhombic space group *Pnma*, with one of the COT^{2-} rings experiencing static disorder over eclipsed and staggered positions with respect to the other. The COT^{2-} rings are not perfectly coplanar, but form a dihedral angle of just 2.8(2)°, significantly less than the 8° dihedral angle observed in ErCp*(COT).[10] The Er−C bond lengths range from 2.575(7) to 2.606(6) Å for the ordered COT^{2-} ring, similar to those reported for $[(N\text{-}^iPr)_2Im][Er(COT)_2]$ though varying over a

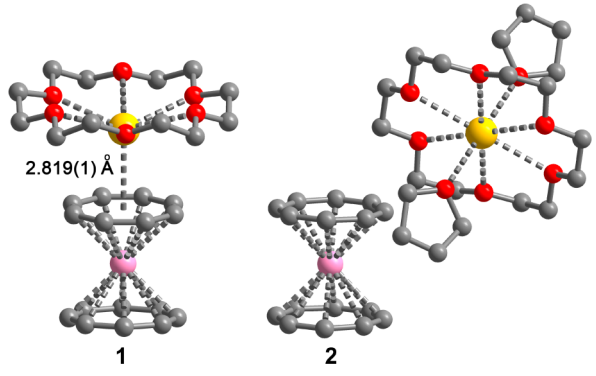

Figure 1. X-ray structures of complexes **1** and **2** with pink, yellow, gray, and red spheres representing Er, K, C, and O, respectively; hydrogen atoms have been omitted for clarity. Two molecules of THF that co-crystallize with each formula unit of **1** are not shown. The upper COT^{2-} ring in **1** is disordered over staggered and eclipsed conformations, while in **2**, the rings are eclipsed with no disorder. The dihedral angles between rings, inter-ring distances, and nearest Er···Er inter-ion distances for **1** and **2**, respectively, are 2.8(2)°/0.00(6)°; 3.730(4) Å/3.749(7) Å; and 7.240(7) Å/7.789(2) Å.

dx.doi.org/10.1021/ja4094814 | J. Am. Chem. Soc. 2013, 135, 17952−17957

smaller range.[17] The Er−COT^{2-} (centroid) distances in **1** are 1.8835(3) and 1.8483(3) Å, identical within error to those in $[(N\text{-}^{i}Pr)_2Im][Er(COT)_2]$.[17]

Dc magnetic susceptibility data were collected for **1** under an applied field of 1000 Oe over the temperature range 1.8−300 K (Figure 2). At room temperature, the value of $\chi_M T$ is 10.9 emu·K/mol, lower than that expected for a $4f^{11}$ configuration with a $J = {}^{15}/_{2}$ ground state (11.48 emu·K/mol). The moment decreases very slightly as the temperature is lowered, until about 10 K where it drops precipitously to a final value of 0.75 emu·K/mol at 1.8 K. This sudden drop in $\chi_M T$ is indicative of magnetic blocking, where a barrier to reorientation of the magnetic moment leads to pinning of the moment along the easy axis within the immobilized crystallites.

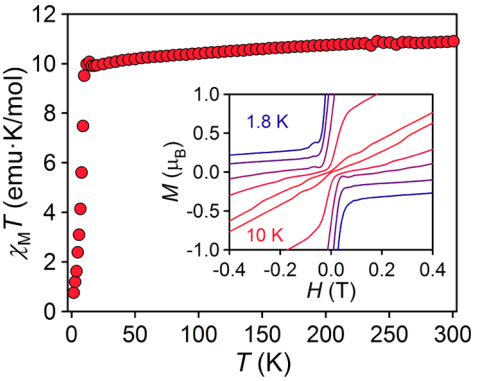

Figure 2. Temperature dependence of the static magnetic susceptibility times temperature ($\chi_M T$) for **1** under an applied field of 1000 Oe. (Inset) Expanded view of the variable-field magnetization for **1** near zero field, revealing hysteresis to 10 K. For all temperatures but 10 K, the loop is open at zero field.

Ac magnetic susceptibility scans collected in the range 1−1500 Hz under zero applied dc field exhibit a single peak in the out-of-phase susceptibility, χ_M'', between 15 and 27 K for **1** (Figure S1). This result is in contrast to ErCp*(COT), which shows two relaxation modes arising from crystallographically distinct disordered conformers.[10] The relaxation time, τ, for **1** at each temperature was extracted by fitting the corresponding plots of χ_M' and χ_M'' using a generalized Debye model.[16] A plot of the natural log of τ versus $1/T$ is linear (Figure S2), suggesting that the relaxation is dominated by the thermally activated Orbach process.[18] Indeed, for all temperatures, the parameter $\alpha \leq 0.08(1)$ indicates a narrow distribution of relaxation times.[16] An Arrhenius fit of the temperature-dependent relaxation time gives a barrier of $U_{eff} = 147(1)$ cm^{-1}, which falls in between the two relaxation barriers of 224.6 and 137.2 cm^{-1} observed for ErCp*(COT). However, a very slight, almost sigmoidal, curvature is apparent in the data and a $\tau_0 = 8.3(6) \times 10^{-8}$ s suggests that the relaxation is not purely Orbach in character.[19] The slight curvature is likely a result of small contributions from additional relaxation mechanisms, as discussed below.

Extrapolating the Arrhenius data for **1** to low temperatures, the relaxation time is 100 s at 10.1 K, suggesting magnetic hysteresis should be apparent below this temperature. Indeed, variable-field magnetization measurements performed up to 3 T revealed a waist-restricted magnetic hysteresis loop from 1.8 to 10 K at a sweep rate of 0.78 mT/s (Figure 2, inset, and Figure S3). The moment plummets to near zero as the field is removed, however, resulting in a coercive field of only 0.7 T at 1.8 K. The remnant magnetization also steadily decreases with increasing temperature, such that for 10 K the loop is closed at zero field. This magnetic hysteresis behavior is reminiscent of that observed for ErCp*(COT), for which the drop in magnetization near zero field was attributed to quantum tunneling of the magnetization.[10]

In an effort to quantify the relaxation at temperatures below the ac range, dc relaxation measurements were carried out at 1.8 K.[8a,10,16] However, instead of an exponential decrease in the magnetization with elapsed time, a drastic drop in the magnetization occurs upon removal of the magnetic field (Figure S4). Such behavior has previously been ascribed to a magnetic avalanche effect, a phenomenon in which heat release upon spin relaxation promotes the relaxation of additional spins.[20] This phenomenon was also identified in the radical-bridged single-molecule magnet $[\{[(Me_3Si)_2N]_2(THF)Dy\}_2(\mu\text{-}\eta^2\text{:}\eta^2\text{-}N_2)]^-$,[8b] and was further well-studied in the archetypal Mn_{12}-acetate single-molecule magnet, wherein it was intimately correlated with tunneling of the magnetization.[21] Indeed, tunneling of the magnetization can trigger the onset of a magnetic avalanche.[22]

Given evidence of a magnetic avalanche through dc relaxation measurements, we sought to determine whether this phenomenon was also contributing to the magnetization drop observed in variable-field measurements. The occurrence of a magnetic avalanche is proposed to be linked to dipolar interactions (cold deflagration),[23] such that dilution of **1** alone might lead to opening of the hysteresis loop. However, as a stand-alone phenomenon, tunneling can lead to loss of remnant magnetization near zero field and be mediated by dipolar interactions.[24] Therefore, we pursued two approaches to identify the precise origins of the drop in the magnetic hysteresis for **1**. As pure tunneling of the magnetization can be facilitated by intrinsic molecular symmetry,[2a,24] we synthesized a salt of $[Er(COT)_2]^-$ in which the sandwich complex is isolated from the potassium counterion, in hopes that tunneling would be minimized in a higher symmetry complex. Additionally, in order to probe the role of dipolar interactions and their impact on both tunneling and a magnetic avalanche, we measured magnetically dilute samples of **1**, prepared with the diamagnetic complex $[Y(COT)_2]^-$.

The compound $[K(18\text{-c-}6)(THF)_2][Er(COT)_2]$ (**2**) was isolated through recrystallization of $K[Er(COT)_2]$ with 2 equiv of 18-crown-6. Only 1 equiv of the crown ether is present in the resulting structure, which crystallizes in the $P\bar{1}$ space group with an outer-sphere potassium counterion encapsulated by an 18-crown-6 and two THF molecules (Figure 1, right). Closely approaching the point group D_{8h}, the molecular symmetry of the $[Er(COT)_2]^-$ complex in **2** is greater than that in **1**, with eclipsed COT^{2-} rings that are nearly coplanar with a dihedral angle of 0.00(6)°. As anticipated given the separation between anion and cation in **2**, the nearest-neighbor Er···Er distance is larger than that in **1** by more than 0.5 Å (Table 1). For **2**, the Er−C bond lengths range from 2.605(3) to 2.632(3) Å, similar to **1** and again close to the range previously reported for $[(N\text{-}^{i}Pr)_2Im][Er(COT)_2]$.[17] Even with these structural differences from **1**, a full examination of **2** through static and dynamic susceptibility measurements reveals the relaxation to be almost indistinguishable between the two complexes (Figures S7−S12). Thus, the slight differences in symmetry appear to play only a minor role in dictating the observed relaxation behavior. Importantly, this result seems to suggest that tunneling between crystal field states due to deviations

dx.doi.org/10.1021/ja4094814 | J. Am. Chem. Soc. 2013, 135, 17952−17957

Table 1. Selected Distances (Å) and Angles (deg) for 1−3

	1	2	3
M···M[a]	7.240(7)	7.789(2)	7.319(1)
Dihedral angle	2.8(2)	0.00(6)	1.642(1)/0.000(2)
M−COT^{2-}[b]	1.87(2)	1.8744(3)	1.9102(0)/1.894(5)
M−C[c]	2.59(1)	2.62(1)	2.64(2)/2.654(7)

[a]Nearest-neighbor distance. [b]Average from COT^{2-} centroid to metal. [c]Average value.

from ideal D_{8h} symmetry is not the sole source of the hysteresis drop. Otherwise, a greater deviation in site symmetry for **1** might be expected to promote very different hysteresis behavior when compared with **2**.

Diluted samples of **1** were prepared in Er:Y molar ratios of 1:20 and 1:85 by co-crystallization with the corresponding Y^{III} compound $[K(18\text{-c-}6)(THF)_2][Y(COT)_2]$ (**3**, Figure S13). Notably, despite crystallization via the same route as **1**, complex **3** crystallizes in the same space group as **2**, namely $P\bar{1}$. Even still, **3** is completely distinct from either Er^{III} complex, with two unique molecules in the unit cell. Despite the lack of an isostructural congener, magnetic dilution with **3** reveals ac relaxation behavior nearly indistinguishable from that of either complex **1** or **2** (vida infra). This is likely due to the fact that each of the unique molecules in **3** possesses metrical parameters very close to **1** or **2** (Table 1), and the ac behavior of the latter two was already shown to be insignificantly influenced by differences in symmetry. Thus, the crystallographic differences do not impede an effective dilution study of the $[Er(COT)_2]^-$ complex. Indeed, for a 1:20 dilution, χ_M'' signal occurs over the same temperature range of 15−27 K as in the concentrated sample (Figure 3, upper) and the relaxation time increases only slightly from **1** or **2** at the lowest temperatures (Tables S1−S3). Fitting the temperature-dependent relaxation data yields $U_{eff} = 150(1)$ cm^{-1} and $\tau_0 = 6.9(5) \times 10^{-8}$ s (Figure 3, lower). Notably, variable-field magnetization data no longer display the same drastic loss at zero field (Figure S16), leading to a near doubling of the remnant magnetization. Dc magnetic relaxation data at 1.8 K suggests that a magnetic avalanche may still be active (Figure S17), although the decline in magnetization with time is now more gradual than in the concentrated sample. Such a change indicates lengthening of the relaxation time at low temperature, which could be attributed to diminished tunneling and also mitigation of a magnetic avalanche.

Relaxation times obtained for a 1:85 dilution of **1** are, within error, the same as those of the 1:20 dilution, although variable-field magnetization data reveal an even further increase in the remnant magnetization (Figure 4). Indeed, at 1.8 K the remnant magnetization and coercive field are 3.53 μ_B and 1.1 T, respectively, and open hysteresis is now observed up to 10 K. The blocking temperature of a single-molecule magnet can be defined either as the maximum temperature for which hysteresis is open at zero applied field (assuming a conventional sweep rate) or the temperature at which the relaxation time is 100 s.[3e,16] In this case, both hysteresis measurements and extrapolation of the relaxation times measured by ac susceptibility result in a blocking temperature of 10 K. Significantly, this represents the highest blocking temperature yet measured for a mononuclear single-molecule magnet, with the previous record of 5 K being held by $Y_{0.95}Er_{0.05}Cp^*(COT)$.[10,25] Even still, at this dilution a small drop in the magnetization close to zero field is observed for all temper-

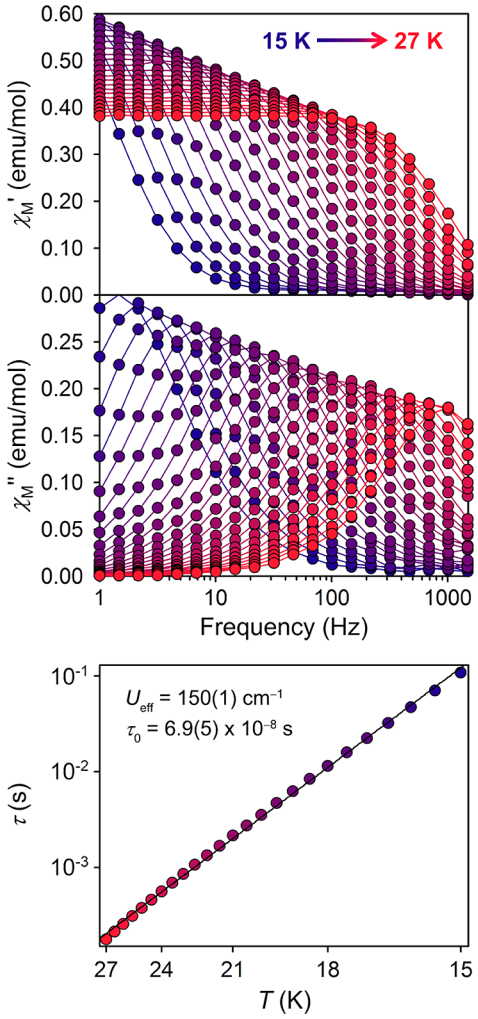

Figure 3. (Upper) Plot of the in-phase (χ_M') and out-of-phase (χ_M'') magnetic susceptibility from 15 to 27 K for a 1:20 (Er:Y) dilution of **1** under zero-applied dc field and a 4 Oe switching field. (Lower) Plot of the relaxation time (τ, log scale) versus T (inverse scale) for a 1:20 (Er:Y) dilution of **1**. A fit to the Arrhenius expression $\ln(\tau) = \ln(\tau_0) + U_{eff}(k_BT)^{-1}$ gives values of $U_{eff} = 150(1)$ cm^{-1} and $\tau_0 = 6.9(5) \times 10^{-8}$ s.

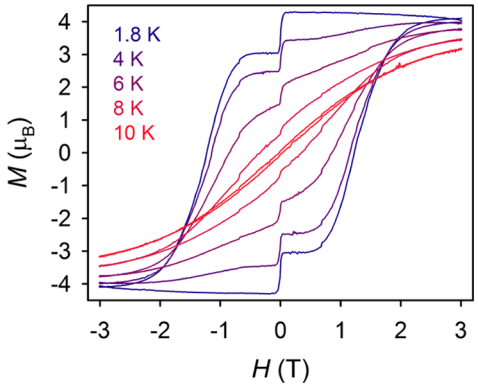

Figure 4. Variable-field magnetization for the 1:85 (Er:Y) dilution of **1**, collected at a sweep rate of 0.78 mT/s. The remnant magnetization and coercive field are 1.5 times greater than in concentrated samples **1** or **2**, a testament to the role of dipolar interactions in the avalanche effect in this system.

dx.doi.org/10.1021/ja4094814 | J. Am. Chem. Soc. 2013, 135, 17952−17957

atures.[26] Given the large separation between magnetic ions, expected to be on average greater than 20 Å,[27] and the knowledge that avalanches can be enhanced or even generated at resonant fields where tunneling occurs,[20,22] we hypothesize that tunneling of the magnetization is the most important remaining mediator of the drop in the hysteresis at this dilution.

We believe that the foregoing results provide evidence of a tunneling-initiated magnetic avalanche in $[Er(COT)_2]^-$, leading to the observed drop in the magnetic hysteresis. Deconvoluting the individual contributions from these two rapid relaxation modes will no doubt require further sophisticated experiments. The role of dipolar interactions is clearly crucial in facilitating both phenomena, however, and a similar conclusion was recently made based on numerical calculations of quantum deflagration in Mn_{12}-acetate.[21d] While this observation alone is not novel, the extensive change in the magnetic hysteresis behavior observed here is one of the more drastic consequences of dilution in the literature. Emphasizing this fact, the 1:20 site dilution of ErCp*(COT) led to opening of the hysteresis loop almost imperceptibly, resulting in a coercive field two orders of magnitude smaller than that achieved here with a 1:20 dilution of $[Er(COT)_2]^-$.[10] Such a pronounced impact of dipolar interactions is reasonable when considering that propagation of a magnetic avalanche is going to depend heavily on heat released by nearby spins.

To gain insight into the specificity of the COT^{2-} ligand field for Er^{III}, we also investigated the magnetic behavior of the compounds $[K(18\text{-c-}6)][Ln(COT)_2]$ (Ln = Sm, Yb, Tb, Dy (**4**), Ho).[14] With the greatest prolate character in their maximal M_J states, the Kramers ions Sm^{III} and Yb^{III} are potential candidates for forming single-molecule magnets in this equatorial ligand field. As non-Kramers ions, Tb^{III} and Ho^{III} are least likely to show zero-field slow relaxation, particularly in this ligand field, due to maximal M_J states that are largely oblate in character.[9] Interestingly, magnetic measurements performed on all of the compounds revealed zero-field slow relaxation only for **4**, at low temperatures with weak thermal dependence (Figures S23−S25). A relaxation barrier of $U_{eff} = 9(1)$ cm^{-1} was extracted by fitting the four highest temperature points in a plot of $\ln(\tau)$ versus $1/T$ (Figure S25), a value which is within range of the 15.6 cm^{-1} determined from ab initio calculations.[12] Although dipolar interactions are likely involved in speeding up the relaxation for **4**, the COT^{2-} ligand field does not engender nearly the same relaxation barrier as obtained for $[Er(COT)_2]^-$. Thus, we believe it is reasonable to infer that the large anisotropy of Dy^{III} and its identity as a Kramers ion contribute most to the observed slow relaxation.

CONCLUSIONS

In summary, the homoleptic Er^{III} sandwich complex in $[K(18\text{-c-}6)][Er(COT)_2]\cdot 2THF$ (**1**) and $[K(18\text{-c-}6)(THF)_2][Er(COT)_2]$ (**2**) has been demonstrated to behave as a single-molecule magnet, much like its heteroleptic predecessor ErCp*(COT),[10] supporting the rationale that the equatorial COT^{2-} ligand field preferentially stabilizes the prolate $M_J = {}^{15}/_2$ state of Er^{III}. In contrast to ErCp*(COT), **1** and **2** demonstrate a single ac feature dominated by thermal relaxation at high temperatures. At low temperatures, relaxation is heavily influenced by dipolar interactions that facilitate tunneling of the magnetization and ultimately trigger a magnetic avalanche, as evidenced by dc relaxation and variable-field magnetization measurements. This result serves as a reminder that the multifaceted role of dipolar interactions in modifying slow relaxation is still being established. Through magnetic dilution, the drop in magnetic hysteresis is largely reduced, leading to magnetic blocking at 10 K. It appears that Er^{III} holds tremendous promise for the design of new single-molecule magnets with even higher blocking temperatures, through the development of stronger equatorial ligand fields than imposed here by a pair of COT^{2-} ligands.

ASSOCIATED CONTENT

Supporting Information

Additional magnetic, structural, and spectroscopic characterization data. This material is available free of charge via the Internet at http://pubs.acs.org.

AUTHOR INFORMATION

Corresponding Author

jrlong@berkeley.edu

Notes

The authors declare no competing financial interest.

ACKNOWLEDGMENTS

We thank the NSF Graduate Fellowship Program for support of K.R.M., Dr. Antonio DiPasquale for assistance with crystal structure determination, and McDonald's Corporation for the drinking straws employed in magnetic sample loading. This research was supported by NSF grant CHE-1111900.

REFERENCES

(1) Ishikawa, N.; Sugita, M.; Ishikawa, T.; Koshihara, S.-y.; Kaizu, Y. *J. Am .Chem. Soc.* **2003**, *125*, 8694.

(2) (a) Ungur, L.; Chibotaru, L. F. *Phys. Chem. Chem. Phys.* **2011**, *13*, 20086. (b) Rajeshkumar, T.; Rajaraman, G. *Chem. Commun.* **2012**, *48*, 7856. (c) Baldoví, J. J.; Borrás-Almenar, J. J.; Clemente-Juan, J. M.; Coronado, E.; Gaita-Ariño, A. *Dalton Trans.* **2012**, *41*, 13705. (d) Baldoví, J. J.; Cardona-Serra, S.; Clemente-Juan, J. M.; Coronado, E.; Gaita-Ariño, A.; Palii, A. *Inorg. Chem.* **2012**, *51*, 12565. (e) Lukens, W. W.; Magnani, N.; Booth, C. H. *Inorg. Chem.* **2012**, *51*, 10105. (f) Chilton, N. F.; Anderson, R. P.; Turner, L. D.; Soncini, A.; Murray, K. S. *J. Comput. Chem.* **2013**, *34*, 1164.

(3) (a) Habib, F.; Lin, P.-H.; Long, J.; Korobkov, I.; Wernsdorfer, W.; Murugesu, M. *J. Am. Chem. Soc.* **2011**, *133*, 8830. (b) Jiang, S.-D.; Liu, S.-S.; Zhou, L.-N.; Wang, B.-W.; Wang, Z.-M.; Gao, S. *Inorg. Chem.* **2012**, *51*, 3079. (c) Tuna, F.; Smith, C. A.; Bodensteiner, M.; Ungur, L.; Chibotaru, L. F.; McInnes, E. J. L.; Winpenny, R. E. P.; Collison, D.; Layfield, R. A. *Angew. Chem., Int. Ed.* **2012**, *51*, 6976. (d) Boulon, M.-E.; Cucinotta, G.; Luzon, J.; Degl'Innocenti, C.; Perfetti, M.; Bernot, K.; Calvez, G.; Caneschi, A.; Sessoli, R. *Angew. Chem., Int. Ed.* **2013**, *52*, 350. (e) Woodruff, D. N.; Winpenny, R. E.; Layfield, R. A. *Chem. Rev.* **2013**, *113*, 5110. (f) Liu, J.-L.; Chen, Y.-C.; Zheng, Y.-Z.; Lin, W.-Q.; Ungur, L.; Wernsdorfer, W.; Chibotaru, L. F.; Tong, M.-L. *Chem. Sci.* **2013**, *4*, 3310. (g) Blagg, R. J.; Ungur, L.; Tuna, F.; Speak, J.; Comar, P.; Collison, D.; Wernsdorfer, W.; McInnes, E. J. L.; Chibotaru, L. F.; Winpenny, R. E. P. *Nat. Chem.* **2013**, *5*, 673. (h) Habib, F.; Brunet, G.; Vieru, V.; Korobkov, I.; Chibotaru, L. F.; Murugesu, M. *J. Am. Chem. Soc.* **2013**, *135*, 13242.

(4) (a) Zadrozny, J. M.; Long, J. R. *J. Am. Chem. Soc.* **2011**, *133*, 20732. (b) Mossin, S.; Tran, B. L.; Adhikari, D.; Pink, M.; Heinemann, F. W.; Sutter, J.; Szilagyi, R. K.; Meyer, K.; Mindiola, D. J. *J. Am. Chem. Soc.* **2012**, *134*, 13651. (c) Zhu, Y.-Y.; Cui, C.; Zhang, Y.-Q.; Jia, J.-H.l; Guo, X.; Gao, C.; Qian, K.; Jiang, S.-D.; Wang, B.-W.; Wang, Z.-M.; Gao, S. *Chem. Sci.* **2013**, *4*, 1802. (d) Zadrozny, J. M.; Xiao, D. J.; Atanasov, M.; Long, G. J.; Grandjean, F.; Neese, F.; Long, J. R. *Nat. Chem.* **2013**, *5*, 577−581.

(5) (a) Rinehart, J. D.; Long, J. R. *J. Am. Chem. Soc.* **2009**, *131*, 12558. (b) Magnani, N.; Colineau, E.; Eloirdi, R.; Griveau, J.-C.; Caciuffo, R.; Cornet, S. M.; May, I.; Sharrad, C. A.; Collison, D.;

Winpenny, R. E. P. *Phys. Rev. Lett.* **2010**, *104*, 197202. (c) Magnani, M.; Apostolidis, C.; Morgenstern, A.; Colineau, E.; Griveau, J.-C.; Bolvin, H.; Walter, O.; Caciuffo, R. *Angew. Chem., Int. Ed.* **2011**, *50*, 1696. (d) Mills, D. P.; Moro, F.; McMaster, J.; van Slageren, J.; Lewis, W.; Blake, A. J.; Liddle, S. T. *Nat. Chem.* **2011**, *3*, 454. (e) Coutinho, J. T.; Antunes, M. A.; Pereira, L. C. J.; Bolvin, H.; Marcalo, J.; Mazzanti, M.; Almeida, M. *Dalton Trans.* **2012**, *41*, 13568. (f) Mougel, V.; Chatelain, L.; Pecaut, J.; Caciuffo, R.; Colineau, E.; Griveau, J.-C.; Mazzanti, M. *Nat. Chem.* **2012**, *4*, 1011. (g) King, D. M.; Tuna, F.; McMaster, J.; Lewis, W.; Blake, A. J.; McInnes, E. J. L.; Liddle, S. T. *Angew. Chem., Int. Ed.* **2013**, *52*, 4921. (h) Moro, F.; Mills, D. P.; Liddle, S. T.; van Slageren, J. *Angew. Chem., Int. Ed.* **2013**, *52*, 3430.

(6) (a) Gonidec, M.; Biagi, R.; Corradini, V.; Moro, F.; De Renzi, V.; del Pennino, U.; Summa, D.; Muccioli, L.; Zannoni, C.; Amabilino, D. B.; Veciana, J. *J. Am. Chem. Soc.* **2011**, *133*, 6603. (b) Ganivet, C. R.; Ballesteros, B.; de la Torre, G.; Clemente-Juan, J. M.; Coronado, E.; Torres, T. *Chem.—Eur. J.* **2013**, *19*, 1457.

(7) Sessoli, R.; Powell, A. K. *Coord. Chem. Rev.* **2009**, *253*, 2328.

(8) (a) Rinehart, J. D.; Fang, M.; Evans, W. J.; Long, J. R. *Nat. Chem.* **2011**, *3*, 538. (b) Rinehart, J. D.; Fang, M.; Evans, W. J.; Long, J. R. *J. Am. Chem. Soc.* **2011**, *133*, 14236. (c) Demir, S.; Zadrozny, J. M.; Nippe, M.; Long, J. R. *J. Am. Chem. Soc.* **2012**, *134*, 18546.

(9) Rinehart, J. D.; Long, J. R. *Chem. Sci.* **2011**, *2*, 2078.

(10) Jiang, S.-D.; Wang, B.-W.; Sun, H.-L.; Wang, Z.-M.; Gao, S. *J. Am. Chem. Soc.* **2011**, *133*, 4730.

(11) Boulon, M.-E.; Cucinotta, G.; Liu, S.-S.; Jiang, S.-D.; Ungur, L.; Chibotaru, L. F.; Gao, S.; Sessoli, R. *Chem.—Eur. J.* **2013**, *19*, 13726.

(12) Le Roy, J. J.; Jeletic, M.; Gorelsky, S. I.; Korobkov, I.; Ungur, L.; Chibotaru, L. F.; Murugesu, M. *J. Am. Chem. Soc.* **2013**, *135*, 3502.

(13) Katz, T. J. *J. Am. Chem. Soc.* **1960**, *82*, 3784.

(14) Hodgson, K. O.; Mares, F.; Starks, D. F.; Streitwieser, A., Jr. *J. Am. Chem. Soc.* **1973**, *95*, 8560.

(15) Bain, G. A.; Berry, J. F. *J. Chem. Educ.* **2008**, *85*, 532.

(16) Gatteschi, D.; Sessoli, R.; Villain, J. *Molecular Nanomagnets*; Oxford University Press: Oxford, 2006.

(17) Jones, P. G.; Hrib, C. G.; Panda, T. K.; Tamm, M. *Acta Crystallogr., Sect. E* **2007**, *63*, m2059.

(18) Orbach, R. *Proc. R. Soc. London, Ser. A* **1961**, *264*, 458.

(19) Attempts to fit the entire temperature regime by accounting for a contribution from Raman relaxation led to a poorer fit than obtained assuming pure Arrhenius behavior.

(20) McHugh, S.; Sarachik, M. P. *Mod. Phys. Lett. B* **2011**, *25*, 1795.

(21) (a) del Barco, E.; Hernandez, J. M.; Sales, M.; Tejada, J.; Rakoto, H.; Broto, J. M.; Chudnovsky, E. M. *Phys. Rev. B* **1999**, *60*, 11898. (b) McHugh, S.; Wen, B.; Ma, X.; Sarachik, M. P.; Myasoedov, Y.; Zeldov, E.; Bagai, R.; Christou, G. *Phys. Rev. B* **2009**, *79*, 174413. (c) Garanin, D. A.; Jaafar, R. *Phys. Rev. B* **2010**, *81*, 180401. (d) Garanin, D. A.; Shoyeb, S. *Phys. Rev. B* **2012**, *85*, 094403.

(22) Suzuki, Y. Magnetic Avalanches in Mn_{12}-acetate, "Magnetic Deflagration". Ph.D. Thesis, City University of New York, New York, NY, 2007.

(23) Sarachik, M. Magnetic Avalanches in Molecular Magnets. In *Molecular Magnets: Physics and Applications*; Bartolomé, J.; Luis, F.; Fernández, J. F., Eds.; Springer: New York, 2014 and references therein.

(24) Gatteschi, D.; Sessoli, R. *Angew. Chem., Int. Ed.* **2003**, *42*, 268.

(25) The single-molecule magnet $[Zn_2DyL_2(MeOH)]NO_3$ (ref 3f; L is the tripodal ligand 2,2′,2″-(((nitrilotris(ethane-2,1-diyl))tris(azane-diyl))tris(methylene))tris-(4-bromophenol)) is reported to show waist-restricted magnetic hysteresis to 11 K. However, the loop is closed at zero field and the data was collected at a sweep rate nearly 2 orders of magnitude faster than that reported here (0.78 versus 20 mT/s) and also the 0.92 and 0.53 mT/s sweep rates reported for ErCp*(COT). Given our definition of blocking temperature as "the maximum temperature for which the hysteresis is open at zero field", we maintain that $[Er(COT)_2]^-$ is the current record holder for highest blocking temperature among mononuclear single-molecule magnets. Ultimately, however, as has been importantly mentioned in ref 3e, the lack of a standard metric for the reporting of M(H) data makes comparison of data across complexes very challenging.

(26) To exclude the possibility that this drop occurs due to inefficient isolation of paramagnetic centers during slow crystallization, we prepared a dilute sample by rapid precipitation (see Supporting Information). Magnetic hysteresis measurements on this sample display a magnetization loss similar to the 1:85 dilution sample (Figure S18).

(27) As estimated from the number of nearest neighbors for complex **3**.